Open Archive TOULOUSE Archive Ouverte (OATAO)

Metabolomic study of fatty livers in ducks: Identification by ^{1}H-NMR of metabolic markers associated with technological quality

Cécile MD Bonnefont,*†‡[1] Aurélie Guerra,*†‡§# Laëtitia Théron,*†‡ Caroline Molette,*†‡
Cécile Canlet,§# and Xavier Fernandez*†‡

*INRA, UMR1289 TANDEM, Chem. de Borde Rouge, 31326 Castanet, France; †Université de Toulouse,
INP ENSAT, UMR1289 TANDEM, av. de l'Agrobiopole, 31326 Castanet, France; ‡INPT ENVT,
UMR1289 TANDEM, Chem. des Capelles, 31076 Toulouse, France; §INRA, UMR1331 TOXALIM,
Chem. de Tournefeuille, 31027 Toulouse, France; and #Université de Toulouse, INP,
UMR 1331 TOXALIM, Chem. de Tournefeuille, 31076 Toulouse, France

ABSTRACT The control of fatty liver fat loss during cooking is a major issue. Previous studies showed that fat loss was influenced by bird production factors and liver technological treatments. However, part of the variability in fat loss remained uncontrolled. To provide enhanced insights into the determinism of fatty liver quality, liver hydrophilic metabolite profiles were measured by nuclear magnetic resonance of the proton (^{1}H-NMR). The study aimed at i) comparing fatty livers with extreme fat loss values and ii) at characterizing the effect of postmortem evolution of livers during chilling. A group of 240 male mule ducks (*Cairina moschata × Anas platyrhynchos*) was reared and overfed. Their livers were sampled at 20 min and 6 h postmortem. Of these birds, 2 groups of ducks were built with extreme values on the technological yield (TY; TY = 100 − % fat loss; the low-fat-loss group, TY = 89.9%, n = 13; and the high-fat-loss group, TY = 68.3%, n = 12, $P <$ 0.001). The ^{1}H-NMR analyses showed that the high-fat-loss livers were more advanced in postmortem biochemical and structural changes than low-fat-loss livers early postmortem. The high-fat-loss livers were characterized by hydrolysis of glycogen into glucose, worse integrity of cell membrane with diminution of compounds of phospholipids, and higher catabolic processes. The accelerated postmortem processes may be the origin of the differences in fat loss during cooking. During the early postmortem period, the adenosine triphosphate amount in liver cells was strongly reduced and lipolysis of triglycerides seemed to be enhanced. The glycogen stored in liver was first converted into glucose, but contrary to what happens in postmortem muscles, glucose was not converted into lactate.

Key words: duck, liver, metabolomics, technological quality

INTRODUCTION

The production of foie gras is mainly localized in France with 74% of the world production in 2011. Most of the production is represented by duck liver, with goose liver accounting for only 2% of the French production of foie gras in 2011. French foie gras is a high-quality standard product with strong added value. Foie gras is a fatty liver induced by overfeeding (JORF, 2006) that results from an intense hepatic lipogenesis from dietary carbohydrates. The lipid contents of fatty livers are greater than 50% in ducks (Chartrin et al., 2006; Théron et al., 2012) and geese (Cazeils et al., 1999). The commercial value of foie gras as a raw material is dependent upon 2 main quality traits: the overall aspect (absence of appearance defects leading to downgrading) and the ability to retain fat during the cooking process. This second trait is regulated by the French market. Fat loss during foie gras cooking must be less than 30% (JORF, 1993). This biological performance is measured by the technological yield (**TY**), which is the ratio between cooked liver weights trimmed of all visible fat and raw liver weights. The first studies on the causes of variation in TY focused on the influence of bird production factors (Baudonnet-Lenfant et al., 1991; Latil et al., 1996), fatty liver technological treatments (Rousselot-Pailley et al., 1992; Bouillier-Oudot et al., 2002), and more recently on the duration of transport and holding in lairage (Fernandez et al., 2011). The liver weight is negatively associated with TY and with the lipid content (Blum et al., 1990;

Rousselot-Pailley et al., 1992). The genetic correlation of fatty liver melting rate (calculated as $100 - TY$) with liver weight, lipid content, and protein content are 0.18, 0.93, and 0.89, respectively, in common duck line (Marie-Etancelin et al., 2011). Nevertheless, a part of the variability of the TY remains uncontrolled (Théron et al., 2011b), and further studies are required to better understand the biological mechanisms underlying the variability in fat loss.

Recently, Théron et al. (2012) modeled TY using several physical and chemical parameters and showed that the optimized model of TY depended on the DM, squared DM, weight, and protein content of fatty livers. Théron et al. (2011b) conducted proteomic analyses to identify protein markers involved in the variability of the TY. They divided a batch of fatty livers into 2 groups, a high-fat-loss group and a low-fat-loss group. Their results suggested that the livers with low-fat-loss during cooking were, at the time of slaughter, still in anabolic processes with regard to energy metabolism and protein synthesis whether the livers with high-fat-loss during cooking developed cell protection mechanisms (Théron et al., 2011b). They also studied the postmortem (**PM**) evolution of these 2 groups during chilling. Their main results suggested lower proteolytic processes during chilling in the low-fat-loss group of fatty livers (Théron et al., 2011b, 2013).

To provide enhanced insights into the differences of cell metabolism in livers with different fat loss capabilities, metabolomic approaches may constitute an interesting tool. Nuclear magnetic resonance of the proton (**^{1}H-NMR**) explorations were chosen because they had the ability to detect all mobile hydrogen-containing metabolites with a simple sample preparation. Because the lipid fraction did not seem to be involved in the determinism of fat loss during cooking (Théron et al., 2012), we decided to focus on the hydrophilic metabolic fraction of fatty liver.

The aim of this study was to determine the role of hydrophilic metabolites in the determination of the level of cooking-induced fat loss. First, we investigated the intrinsic characteristics of livers at time of slaughter, and then focused on the effects of PM chilling on liver metabolic profile. This work completes the study of Théron et al. (2011b) on the protein fraction in the same samples. This study also enables to characterize the fatty liver metabolome; to our knowledge it is the first study of the hydrophilic metabolite profiles of fatty liver by ^{1}H-NMR analyses.

MATERIALS AND METHODS

Bird Management and Fatty Liver Processing

The ducks were bred and overfed in the same conditions as in commercial farms. All details about bird breeding, overfeeding, and slaughter are available in Théron et al. (2011b). Briefly, 240 male mule ducks (*Cairina moschata × Anas platyrhynchos*) of a commercial strain were reared collectively with access to free range until 13 wk. They could access to an outside field from 6 to 13 wk. During this period, they were bred in natural light and temperature conditions. At 13 wk, they were overfed in collective confinement for 12 d with soaked-corn mixture (42% of grain – 58% of flour) twice a day. They were then weighed and slaughtered 10 h after the last meal. Birds were rendered unconscious by electrical stunning and bled by ventral cutting of neck vessels. The experiments described here fully comply with legislation on research involving animal subjects according to the European Communities Council Directive of November 24, 1986 (86/609/EEC). Investigators were certificated by the French governmental authority for carrying out these experiments (agreement n°31–11.43.501).

At the end of the slaughter process, 20 min after bleeding, livers were removed from the carcasses and weighted. Their pH was measured using penetration electrode with portable pH meter (Eutech Instruments, Singapore). The color characteristics were measured using the trichromatic CIE Lab coordinate system (L*, a*, and b*) with a CR 300 Minolta chromameter (Osaka, Japan). The livers were chilled on ice during 6 h. The main blood vessels were carefully removed. Two samples of around 20 g were taken off in the upper part of the main lobe of the liver at 20 min and 6 h PM. They were dropped into liquid nitrogen and stored vacuum packed at $-80°C$ for ^{1}H-NMR analyses. After the 6 h of chilling, a slice of approximately 180 g was excised perpendicular to the long axis of the liver and across the large and small lobes. It was put into a glass jar with salt and pepper (12 and 2 g/kg, respectively). The jars were cooked during 1 h in water at 85°C (pasteurize value = 170 min). The jars were stored at 4°C. Two months after, they were opened and all the visible fat exuded during cooking was carefully removed from the fatty liver. The TY was evaluated as the ratio between cooked liver weights trimmed of all visible fat and raw liver weights and expressed as a percentage.

Biochemical Analyses

Biochemical analyses were realized on the fatty livers that were sampled at 6 h PM. The first samples were ground into fine powder. Dry matter was determined by desiccation of fatty liver powder in an oven at 105°C for 24 h (JOCE, 1971). Total lipids were extracted from the fatty liver powder by homogenization in chloroform methanol 2:1 (vol/vol) and measured gravimetrically according to the method of Folch et al. (1957).

The fatty liver characteristics of all male mule ducks (n = 240) are presented in the Table 1. Of these samples, 2 groups were built with extreme TY (the low-fat-loss group: TY = 89.9%, n = 13 and the high-fat-loss group: TY = 68.3%, n = 12) and equivalent fatty liver

Table 1. Characteristics of ducks and fatty livers in the entire batch and in the 2 fat loss groups (means ± SEM)

Item	Batch samples (n = 240)	Low-fat-loss group (n = 13)	High-fat-loss group (n = 12)	t-Test of the fat loss group effects
Technological yield, %	78.9 ± 13.9	89.9 ± 0.8	68.3 ± 1.3	***
Bird weight at slaughter, g	6,287 ± 339	6,281 ± 72	6,198 ± 92	0.500
Fatty liver weight,[1] g	546 ± 96	570 ± 8	582 ± 9	0.328
Lipid content,[2] %		55.8 ± 0.8	55.6 ± 1.5	0.933
DM,[2] %	67.9 ± 3.2	67.7 ± 0.3	68.9 ± 0.6	0.105
pH[1]	5.91 ± 0.11	5.90 ± 0.02	5.84 ± 0.03	0.139
L*[1]	64.3 ± 2.7	64.9 ± 0.3	62.6 ± 2.2	0.318
a*[1]	8.5 ± 1.1	8.7 ± 0.2	8.2 ± 0.2	0.242
b*[1]	33.0 ± 2.4	33.3 ± 0.4	33.9 ± 0.5	0.423

[1]At 20 min postmortem. Trichromatic CIE Lab coordinate system (L*, a*, and b*).

[2]At 6 h postmortem.

***$P < 0.001$.

weight and lipid content (Table 1). Afterward, studies focus on the comparison of these 2 groups of fatty livers with low-fat-loss and high-fat-loss during cooking.

Glycogen and free glucose were measured at 20 min and 6 h PM. About 1 g of frozen fatty liver powder was homogenized into 15 mL of 0.5 M perchloric acid. After removal of the fat cake, two 0.5-mL aliquots of the homogenate were sampled. The first aliquot was centrifuged (20 min at 2,500 × g at 4°C) and its supernatant was used for free glucose and lactic acid determination (Bergmeyer, 1974). In the second aliquot, glycogen was hydrolyzed with amyloglycosidase (Dalrymple and Hamm, 1973) and total glucose was measured by enzymatic determination as described previously. The glycogen content was determined as the difference between the content of glucose after glycogen hydrolysis and the content of free glucose. All the carbohydrate contents were expressed as micromoles per gram of fat free liver weight.

Hydrophilic Metabolite Extraction

The metabolomic analyses focused on the hydrophilic fraction of the liver cells. A method adapted from Beckonert et al. (2007) enabled the separation of hydrophilic and lipophilic metabolites by a water-methanol-chloroform mix. The hydrophilic metabolites of the 25 fatty livers sampled at 20 min PM and at 6 h PM (n = 49, one sample of the high-fat-loss group sampled at 6 h PM was missing) were extracted. Briefly, a sample of 0.5 g of fatty liver homogenized into powder was mixed into 4 mL of methanol and 2 mL of water with a Polytron for 30 s at 19,000 rpm. Four milliliters of chloroform and 2 mL of water were added. After 15 min at 4°C, the mix was centrifuged at 1,000 × g at 4°C for 15 min. The centrifugation activated the mix separation into 2 phases. The upper phase was composed of water and methanol with hydrophilic metabolites, whereas the chloroform in the lower phase contained the lipids. Proteins and other amphiphilic molecules formed a fat cake between the 2 phases. The upper phase was cautiously sampled for NMR analysis. It was then evaporated with a Speedvac (vacuum concentrator, Thermo Fisher Scientific, San Jose, CA) at 6 Torr to eliminate methanol and water and stored at −20°C.

Sample Preparation for ^{1}H-NMR

The samples were then diluted into 800 µL of deuterated water (D_2O) with sodium trimethylsilylpropionate (TMSP, 10 mg of TMSP into 100 mL of D_2O) and centrifuged at 4,600 × g at 4°C. A volume of 600 µL was sampled and transferred into NMR tubes.

All ^{1}H-NMR spectra were obtained using a Bruker DRX-600 Avance NMR spectrometer operating at 600.13 MHz for a ^{1}H resonance frequency and an inverse detection 5 mm [1]H-[13]C-^{15}N cryoprobe. They were acquired at 300 K using the Carr-Purcell-Meiboom-Gill spin-echo pulse sequence with presaturation and a total spin-echo delay (2 nτ) of 240 ms to attenuate broad signals from proteins and lipoproteins. A total of 128 transients were collected into 32 K data points using a spectral width of 20 ppm, a relaxation delay of 2 s, and an acquisition time of 1.36 s. Prior to Fourier transformation, an exponential line broadening function of 0.3 Hz was applied to the free induction decay. All spectra were manually phased and baseline corrected using Topspin (V2.1, Bruker, Biospin, Munich, Germany). They were referenced to TMSP at 0 ppm. They were then data reduced using AMIX software (version 3.9, Bruker Biospin) to integrate 0.01 ppm wide regions corresponding to the δ 10 to 0.5 ppm regions. Some buckets were removed because they contained contaminants (1.175–1.195 ppm for ethanol, 3.30 to 3.40 ppm for methanol, 4.40 to 5.10 ppm for water, and a nonidentified bucket at 7.65 ppm that was present on the test tubes). The peak of glycogen (5.40 ppm) was also eliminated as this metabolite precipitated in the methanol and chloroform that were used for the extraction. Each integrated region was normalized to the total intensity of spectrum to generate quantitative variables. A total of 900 buckets were included in the data matrices.

To confirm the chemical structure of metabolites of interest, 2D ^{1}H-^{13}C-HSQC (heteronuclear single quantum coherence spectroscopy) NMR experiment was performed on one sample.

Statistical Analyses of the Hydrophilic Metabolites by ^{1}H-NMR

Statistical analyses were performed with SIMCA P+ software (version 12, Umetrics, AB, Umea, Sweden) to identify i) the buckets that discriminated the low-fat-loss fatty livers and the high-fat-loss fatty livers at the time of slaughter (20 min PM) and ii) the buckets whose intensity changed during chilling (6 h PM vs. 20 min PM). Filtered data were mean-centered and scaled (Pareto). First, a principal component analysis (**PCA**) was performed to observe data and eliminate outlier samples. Then the orthogonal projection of latent structures–discriminant analysis (**OPLS-DA**) supervised method was performed. The OPLS-DA is similar to PCA but uses discriminant variables that correlate to class membership. It permits better discrimination of 2 groups. The axes represent the latent variables. Discriminant buckets were determined using variable importance in projection (**VIP**), an appropriate quantitative statistical parameter ranking the buckets according to their ability to discriminate different groups. The buckets were referenced by their chemical shift, expressed in ppm. The performance of the OPLS-DA model was evaluated by R^2Y and Q^2 parameters, which informed about the explained variance and the predictive ability of the model, respectively. All OPLS-DA models were constructed using a 7-fold cross-validation method to determine the number of latent variables to include in the OPLS-DA model and further assessed with a 200-permutation test to calculate the robustness and validity of the OPLS-DA results. For each bucket, the significance was checked by a one-by-one ANOVA with the group effect. The *P*-values were corrected for multiple test with the false discovery rate (Hochberg and Benjamini, 1990) using the R software (version 2.14.1). The low-fat-loss group to high-fat-loss group intensity ratio was calculated to analyze the group effect and the 6 h to 20 min intensity ratio was calculated to analyze the PM effect.

Discriminant buckets were identified by matching 1D (^{1}H-NMR) and 2D (^{1}H-^{13}C NMR) data to reference spectra in a homemade reference database, as well as with other databases (http://www.bmrb.wisc.edu/; http://www.hmdb.ca/), and reports in the literature. Few buckets were assessed to 2 or more metabolites, so they are not discussed in this paper.

Biological Interpretation of the Focus Metabolites

The focus metabolites were analyzed using IPA (Ingenuity Systems, http://www.ingenuity.com) through HMDB annotation (Human Metabolome Database). The network analysis was performed with only direct links between 2 metabolites, and a score was calculated for the significance of the network. The higher the score, the more significant the network. IPA function

analyses were also performed. The significance of the association between the list of metabolites and different functions was measured by Fisher's exact test. Only the functions with at least 4 metabolites and a *P*-value less than 10^{-4} were kept in this study.

RESULTS AND DISCUSSION

The aim of this study was to determine the role of intrinsic liver characteristics at the time of slaughter and the role of PM evolution during the chilling in the establishment of fat loss during cooking.

First, 2 groups of ducks were built with extreme TY values. The TY of the low-fat-loss group (n = 13) was strongly higher than that of the high-fat-loss group (n = 12) with 89.9 and 68.3%, respectively ($P < 0.001$; Table 1). The bird weights were equivalent, 6,281 and 6,198 g, respectively ($P = 0.500$). Their fatty liver weights were also equivalent, 570 and 582 g, respectively ($P = 0.328$). The lipid contents, DM rates, pH values, and color values (L*, a*, and b*) did not differ significantly between the groups (Table 1).

Comparison of the Low-Fat-Loss and High-Fat-Loss Fatty Livers at the Time of Slaughter

The ^{1}H-NMR spectra of the livers sampled at 20 min PM were first analyzed by PCA. One outlier sample from the high-fat-loss group was removed. The PCA could not separate the 2 groups (plot not shown). An OPLS-DA supervised analysis was then performed to maximize the variance between the 2 groups. It succeeded in separating the high-fat-loss samples from the low-fat-loss samples with the first latent variable (Figure 1A). The relevance (R^2Y) and prediction (Q^2) values of the model were 0.681 and 0.467, respectively. The real R^2Y and Q^2 values were largely greater than the values obtained after 200 permutations, meaning that the OPLS-DA model was significant (data not shown). The annotated loading plot of this model is presented in Figure 1B.

A total of 59 buckets were considered as significant as they had a VIP value greater than 2 in the OPLS-DA analysis (arbitrary threshold used, Table 2). Among the 59 significant buckets, 52 could be annotated. Six metabolites were less abundant in the low-fat-loss group than in the high-fat-loss group because they had a low-fat-loss group to high-fat-loss group intensity ratio less than 1. The glucose was represented by 8 buckets with VIP values between 2.08 and 3.75. Five of them were significant (buckets at 3.255, 3.485, 3.885, 3.905, and 5.225 ppm), 2 tended to be significant ($P = 0.064$ and $P = 0.098$, for the buckets at 3.725 and 3.535, respectively), and 1 was not significant ($P = 0.133$, bucket at 3.465 ppm; Table 2). The lactate was represented by 4 buckets at 1.315, 1.325, 1.335, and 4.125 ppm and 2 of them had the highest VIP values (greater than 5 units)
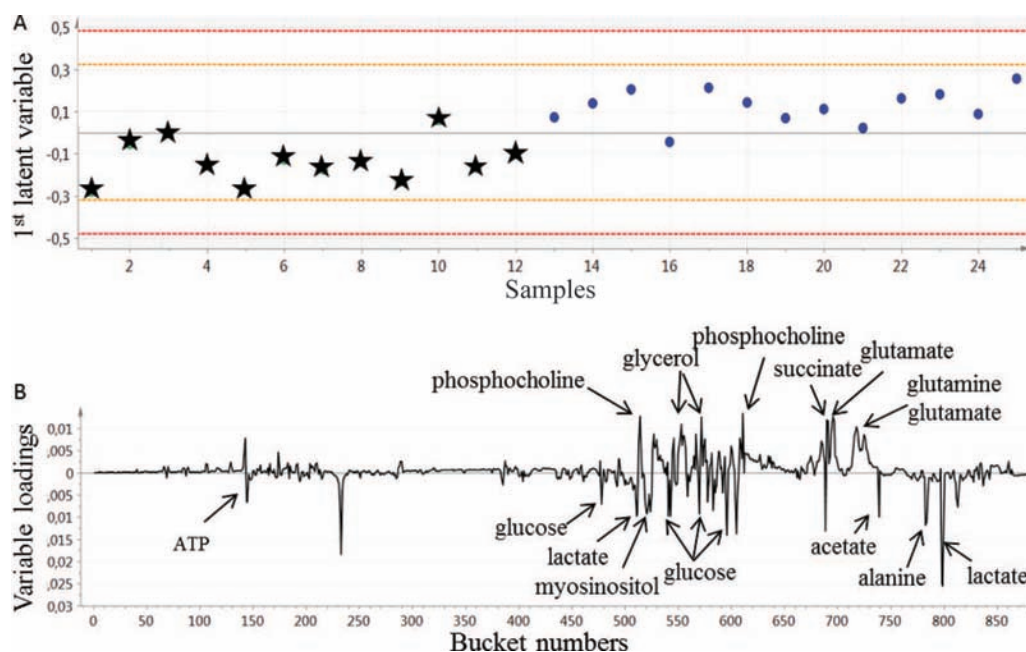
Figure 1. One-dimensional orthogonal projection of latent structures–discriminant analysis score plot of the fat loss groups before chilling integrated ^{1}H-NMR spectra. The low-fat-loss livers are represented by circles (n = 13) and the high-fat-loss livers by stars (n = 12; at 20 min postmortem). Relevance (R^2Y) = 0.681, and prediction (Q^2) = 0.467. A: Score plot and B: loading plot. Color version available in the online PDF.

even if their P-values were 0.074 and 0.093, respectively. Their ratios were between 0.78 and 0.92 (Table 2). The lower concentration of glucose in the low fat-loss livers was not confirmed by carbohydrate biochemical measures as the ratio was 1.08. The free glucose was higher in the low-fat-loss livers than in the high-fat-loss livers (43.5 and 40.2 µmol/g of fat free liver, respectively, P = 0.067). The glycogen tended to be higher in the low-fat-loss group than in the high-fat-loss group (227.1 and 197.1 µmol/g of fat free liver, respectively, P = 0.109).

The higher amount of glycogen (shown by enzymatic analyses) and the lower content of glucose (shown by ^{1}H-NMR analyses) in the low-fat-loss livers indicated i) that glycogen storage was higher in this group, ii) that the hydrolysis of glycogen into glucose was enhanced in the high-fat-loss group, or both i and ii.

The samples were taken off 20 min after duck slaughter, thus PM processes may have begun. It is well known in muscle that PM changes lead to a decrease in glycogen content, an accumulation of lactate, and a decrease in the pH (Bendall, 1979). Here the pH of the livers did not differ significantly between the groups (pH = 5.90 in the low-fat-loss livers, pH = 5.84 in the high-fat loss liver, P = 0.14, Table 1). However, the carbohydrate contents showed that at 20 min PM the high-fat-loss livers had later PM evolution than the low-fat-loss livers. Théron et al. (2011b) studied the proteome of the same livers, and showed that the livers with low fat loss during cooking were still in anabolic processes. The results of proteome and metabolome match and show that in the early PM period the PM evolution is more advanced in the high-fat-loss livers.

The protein metabolism was also affected by the groups. Two buckets of the alanine (at 1.475 and 1.485 ppm) had VIP values greater than 3.1 and P-values less than 0.05. Their ratios were around 0.82 (Table 2). The buckets at 3.265 and 3.275 ppm that corresponded to either betaine or taurine had VIP values of 5.96 and 2.98, and P-values less than 0.01 and equal to 0.092, respectively (Table 2). The ratios were around 0.9. Among amino acids, alanine was the most effective precursor for gluconeogenesis (Yamamoto et al., 1974). Both betaine (Barak et al., 1997; Neuschwander-Tetri, 2001) and taurine (Klein et al., 2011) were increased in alcoholic and nonalcoholic hepatic steatosis because they had a role in cell protection mechanisms. Whatever the amino acid identified in the buckets at 3.265 and 3.275 ppm (taurine or betaine), they could be used as molecular markers of liver steatosis.

The acetate was also identified by its singlet in the bucket at 1.925 ppm. It had a VIP value of 3.43 and a ratio of 0.79 (Table 2). The acetate contributed to the suppression of lipogenesis in liver (Yamashita et al., 2009) and to the upregulation of genes involved in fatty acid oxidation (Kondo et al., 2009). However, here, the lipid content in the 2 groups of liver did not differ significantly (Table 1), so the group differences could not be interpreted as fattening differences.

On the contrary, 7 significant metabolites were more abundant in the low-fat-loss group than in the high-fat-loss group since they had a ratio greater than 1. The choline, phosphocholine, and glycerophosphocholine were represented by 1 (at 3.205 ppm), 3 (from 4.165 to 4.185 ppm), and 1 bucket (at 3.225 ppm), respectively. The VIP values of all these buckets were greater than 3.

Table 2. List of the buckets that discriminate the low-fat-loss group (n = 13) and the high-fat-loss group (n = 12) at 20 min post-mortem [variable importance in projection (VIP) >2][1,2]

Chemical shift	Metabolite	HMDB annotation	Multiplet[3]	Ratio[4]	VIP	P[5]
8.575	Unknown compound		s	2.51	2.49	**
4.015	Unknown compound		m	1.22	2.73	***
4.025	Unknown compound		m	1.22	2.2	***
4.165	Phosphocholine		m	1.63	2.16	**
4.175	Phosphocholine		m	1.59	4.11	***
4.185	Phosphocholine		m	1.23	2.96	*
3.205	Choline	HMDB00097	s	1.25	4.13	**
3.225	Glycerophosphocholine	HMDB00086	s	1.07	4.22	0.285
2.405	Succinate	HMDB00254	s	1.62	3.1	*
2.415	Succinate	HMDB00254	s	1.12	4.19	*
3.595	Myo-inositol	HMDB00211	m	1.27	4.07	***
4.045	Myo-inositol	HMDB00211	t	1.41	2.53	**
4.055	Myo-inositol/choline	HMDB00211/HMDB00097	t	1.1	2.07	0.054
3.615	Myo-inositol/glucose/glycerol/lysine	HMDB00211/HMDB00122 /HMDB00131/HMDB00182	m	0.93	2.2	0.086
2.345	Glutamate	HMDB00148	m	1.18	3.28	**
2.355	Glutamate	HMDB00148	m	1.17	3.66	**
2.365	Glutamate	HMDB00148	m	1.15	3.18	**
2.375	Glutamate	HMDB00148	m	1.15	2.51	**
2.055	Glutamate/proline	HMDB00148/HMDB00162	m	1.14	2.15	**
2.065	Glutamate/proline	HMDB00148/HMDB00162	m	1.15	2.45	**
2.125	Glutamine/glutathione	HMDB00641/HMDB00125	m	1.19	2.55	*
2.135	Glutamine/glutathione	HMDB00641/HMDB00125	m	1.18	2.61	0.084
2.145	Glutamine/glutathione	HMDB00641/HMDB00125	m	1.16	2.36	0.116
2.155	Glutamine/glutathione	HMDB00641/HMDB00125	m	1.16	2.36	*
2.165	Glutamine/glutathione	HMDB00641/HMDB00125	m	1.11	2.13	*
3.765	Glucose, alanine, glutamine, glutathione, glutamate	HMDB00122/HMDB00161 /HMDB00641/HMDB00129 /HMDB00148	m	1.06	2.54	*
3.775	Glucose, alanine, glutamine, glutathione, glutamate	HMDB00122/HMDB00161 /HMDB00641/HMDB00129 /HMDB00148	m	1.03	2	0.099
3.785	Glucose, alanine, glutamine, glutathione, glutamate	HMDB00122/HMDB00161 /HMDB00641/HMDB00129 /HMDB00148	m	1.09	3.9	**
3.235	Glucose, arginine	HMDB00122/HMDB00517	t	1.04	2.51	0.508
3.855	Glucose, serine	HMDB00122/HMDB00187	m	1.05	2.25	0.095
3.645	Glycerol	HMDB00131	m	1.09	2.92	*
3.795	Glycerol	HMDB00131	m	1.1	2.83	**
3.805	Glycerol	HMDB00131	m	1.13	2.23	***
3.565	Glycerol/glycine	HMDB00131/HMDB00123	m	1.1	2.56	*
3.755	Lysine	HMDB00182	m	1.05	2.14	0.056
1.475	Alanine	HMDB00161	d	0.84	3.18	*
1.485	Alanine	HMDB00161	d	0.8	3.74	*
1.925	Acetate		s	0.79	3.43	**
8.565	ATP, ADP	HMDB00538	s	0.3	2.33	**
3.255	Glucose	HMDB00122	t	0.91	3.17	**
3.465	Glucose	HMDB00122	m	0.95	2.09	0.133
3.485	Glucose	HMDB00122	m	0.92	3.67	*
3.535	Glucose	HMDB00122	m	0.94	2.08	0.098
3.725	Glucose	HMDB00122	m	0.95	2.3	0.064
3.885	Glucose	HMDB00122	m	0.94	3.11	*
3.905	Glucose	HMDB00122	m	0.93	3.75	***
5.225	Glucose	HMDB00122	d	0.84	2.78	**
1.315	Lactate	HMDB01311	d	0.78	2.8	*
1.325	Lactate	HMDB01311	d	0.89	5.92	0.074
1.335	Lactate	HMDB01311	d	0.9	5.63	0.093
4.125	Lactate	HMDB01311	q	0.92	2.06	*
4.195	Phosphocholine, ATP		m	0.83	2.13	0.103
4.205	Phosphocholine, ATP		m	0.63	2.72	**
3.265	Taurine/betaine	HMDB00251/HMDB00043	t/s	0.86	5.96	**
3.275	Taurine/betaine	HMDB00251/HMDB00043	t/s	0.92	2.98	0.092
4.075	Unknown compound		t	0.7	2.63	**
2.425	Unknown compound		s	0.46	4.06	**
7.685	Unknown compound		s	0.42	2.37	0.255
7.675	Unknown compound		s	0.24	5.48	0.179

[1]HMDB = Human Metabolome Database; ATP = adenosine triphosphate; ADP = adenosine diphosphate.

[2]The R^2Y and Q^2 values of the model were 0.681 and 0.467, respectively.

[3]Multiplet indicates the peak form on the ^{1}H-NMR spectra, s for singlet, d for doublet, t for triplet, and m for multiplet.

[4]Ratio represents the low-fat-loss group to the high-fat-loss group ratio.

[5]P is the FDR-corrected P-value of the ANOVA of the fat loss group effect.

***$P < 0.001$, **$0.001 \leq P < 0.01$, *$0.01 \leq P < 0.05$.

Their ratios were between 1.07 and 1.63 (Table 2). All buckets were significant ($P < 0.05$), except the bucket of glycerophosphocholine ($P = 0.285$). These metabolites are involved in the synthesis of phospholipids that are the main membrane constituents. The higher concentration of these metabolites in the low-fat-loss livers could display better integrity of the membranes, in relationships with the higher retention of lipids during cooking.

The myo-inositol was represented by 2 buckets (at 3.595 and 4.045 ppm). These buckets had VIP values of 4.07 and 2.53, respectively, and they were significant ($P < 0.05$). Their ratios were between 1.27 and 1.41 (Table 2). The absence of myo-inositol in the diet of rats leads to an accumulation of lipids (Beach and Flick, 1982). Mice treated with myo-inositol exhibited a decrease in white adipose tissue accretion due to a decrease in adipose cell volume (Croze et al., 2013). The higher myo-inositol contained in the low-fat-loss livers might be related to the smaller size of lipid droplets as evidenced by Théron et al. (2011a).

The protein metabolism was also strongly affected. Two buckets stood for the succinate (at 2.405 and 2.415 ppm); their VIP values were greater than 3 and their P-values were less than 0.05. Their ratios were between 1.12 and 1.62 (Table 2). The succinate reduces oxidative stress and improves mitochondrial function in mice with steatotic livers (Evans et al., 2009). The higher amount of succinate in the high-fat-loss livers meant that oxidative stress was activated and that cells triggered protection mechanisms. This result matches with previous observations (Théron et al., 2011b).

The glutamate family was well represented with 4 buckets for the glutamate (from 2.345 to 2.375 ppm) and 5 buckets for glutamine, glutathione, or both (from 2.125 to 2.165 ppm). The VIP values were between 2.13 and 3.66, and the P-values were significant except for 2 buckets ($P = 0.084$ and 0.116, for the peaks at 2.135 and 2.145 ppm, respectively). Their ratios were between 1.11 and 1.19 (Table 2). In pork, the diminution of glutamate content and the increase of alanine in PM muscles indicate a proteolytic profile associated with meat aging (Lopez-Bote et al., 2008). The lower concentration of glutamate and the higher concentration of alanine in the high-fat-loss livers show an increase in protein degradation, which confirms previous results (Théron et al., 2011b).

The glycerol was represented by 3 buckets (at 3.645, 3.795, and 3.805 ppm) with VIP values greater than 2.2 and P-values less than 0.05 and by 1 bucket (at 3.565 ppm) that corresponded to glycerol, glycine, or both (Table 2). Their ratios were around 1.1. The glycerol is released from triglyceride during lipolysis. The higher amount of glycerol in the high-fat-loss livers was likely due to a higher lipolysis even if the lipid content in both groups was equivalent (Table 1). This indicates that the metabolite profiles are different between the 2 groups. The livers in the high-fat-loss group must be in

a regression evolution with lipolysis contrary to livers from the low-fat-loss livers. This hypothesis strengthens the hypothesis that livers in the low-fat-loss group are still in anabolic processes (Théron et al., 2011b).

To better understand the biological interpretation of the differences of metabolisms between the low-fat-loss and high-fat-loss livers, data were also analyzed with IPA software (Ingenuity Systems, www.ingenuity.com). After HMDB annotation, only 14 metabolites were recognized by IPA software. The network analysis highlighted one network (Figure 2) that gathered 10 of the 14 focus metabolites and that scored 24. The IPA function analysis highlighted 37 functions with at least 4 molecules and with a P-value less than 10^{-4}. Of the 37 functions, 16 were directly involved in amino acid metabolism, through the transport of amino acids, the uptake of amino acids, and protein synthesis ($1.9 \times 10^{-8} < P < 10^{-4}$; data not shown). This result showed that protein metabolism was determinant for fat loss during cooking. The conversion of lipids and liver steatosis were also significant with 7 metabolites [adenosine triphosphate (**ATP**), glucose, glutathione, glutamic acid, glutamine, lysine, taurine, $P = 3.13 \times 10^{-5}$] and 4 metabolites (betaine, choline, glutamic acid, and taurine, $P = 4.73 \times 10^{-5}$), respectively. These results were expected because the liver is the main organ involved in lipogenesis.

Metabolic Changes of Fatty Livers During Chilling

The second step of this study analyzed the effect of PM changes during the fatty liver chilling. To mimic the duration of chilling in slaughter industries, the fatty livers sampled at 20 min were chilled on ice for 6 h. During that operation, the liver core temperature fell from 41°C to approximately 4°C.

The ^{1}H-NMR spectra were first analyzed by PCA, and 1 outlier sample was eliminated (data not shown). An OPLS-DA analysis was performed to search markers that discriminated between the 2 PM times. The separation between the groups was very clear in the horizontal axis (1st latent variable, Figure 3A). The R^2Y and Q^2 values for the first latent variable were 0.978 and 0.968, respectively. The loading plot of this model is presented in the Figure 3B.

A total of 55 buckets had VIP values greater than 2 and all of them were very significant ($P < 0.001$, Table 3). A total of 38 buckets had a 6 h PM to 20 min PM intensity ratio greater than 1, meaning that their relative proportion increased during chilling.

The glucose was represented by 12 buckets (from 3.445 to 3.875 and at 5.235 ppm). All these buckets were very significant ($P < 0.001$) and the VIP values ranged between 2.27 and 4.42. The ratios were between 1.15 and 1.76 (Table 3). The carbohydrate biochemical measures confirmed this result as the amounts of free glucose increased from 41.9 to 63.7 μmol of free
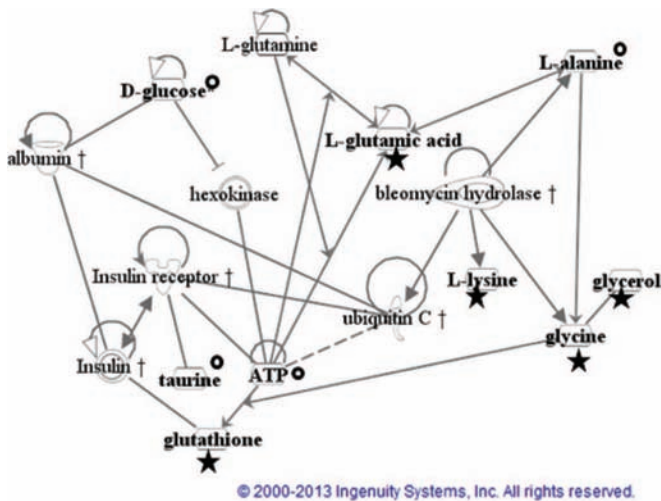
Figure 2. Ingenuity network of the fat loss groups before chilling integrated ^{1}H-NMR spectra. The metabolites identified with the orthogonal projection of latent structures–discriminant analysis of the low-fat-loss and high-fat-loss groups sampled at 20 min postmortem (n = 25) were analyzed with Ingenuity (http://www.ingenuity.com). The network involves 10 of the 14 annotated metabolites and scores 24. The metabolites upregulated in the low-fat-loss group are represented with a circle and the metabolites upregulated in the high-fat-loss group are symbolized with a star. The main functions of this network are amino acid metabolism, molecular transport, and small molecule biochemistry. Seventeen metabolites were directly linked to both adenosine triphosphate and ubiquitin, they were replaced by the dotted line between these metabolites. Color version available in the online PDF.

glucose/g of fat free liver between 20 min and 6 h PM ($P < 0.001$). In parallel, the glycogen amounts decreased strongly from 213.3 to 152.2 µmol/g of fat free liver ($P < 0.001$). This result shows that during PM evolution a fraction of glycogen is converted into glucose in the liver.

The glycerol was represented by 5 buckets (from 3.565 to 3.795 ppm) with VIP values between 2.07 and 4.58. The ratios were between 1.21 and 1.56 (Table 3). The increase in glycerol proportion during chilling might be due to lipolysis of triglycerides.

On the contrary, 17 buckets had a decreasing intensity during the time course of the chilling; their relative proportion was higher at 20 min PM than at 6 h PM. They were mainly characterized by 3 metabolites, lactate, phosphocholine, and glycerophosphocholine.

The lactate was represented by 4 significant buckets (at 1.325, 1.335, 4.105, and 4.115 ppm). The 2 first ones had VIP values around 2.35 and the other ones around 4.35. The ratios were around 0.78 (Table 3). In PM muscles, the anaerobic glycolysis leads to the increase in lactate content and the subsequent diminution of pH (Sharp, 1935). On the contrary, the lactate decreased in the liver. Here, the results indicate that during PM evolution of the liver, the glycogen is converted into glucose but the glucose is not converted into lactate. The phosphocholine and the glycerophosphocholine were represented by 1 (at 3.225 ppm) and 3 significant buckets (at 3.235, 4.325, and 4.335 ppm), respectively. The VIP values were very high for 2 buckets (greater than 5.5 at 3.235 and 3.225 ppm) and slightly greater
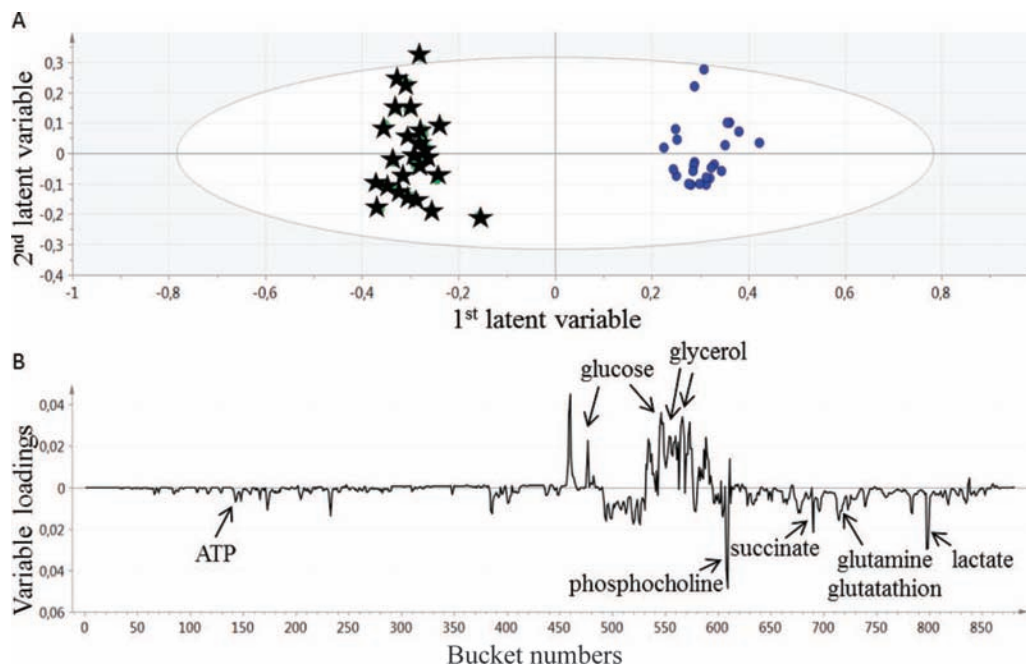

Figure 3. Two-dimensional orthogonal projection of latent structures–discriminant analysis score plot of the fatty livers during chilling integrated ^{1}H-NMR spectra. The fatty livers sampled at 20 min postmortem are represented by stars (n = 25) and the ones sampled at 6 h postmortem are represented by circles (n = 24). Relevance (R^2Y) = 0.978, and prediction (Q^2) = 0.968. A: Score plot and B: loading plot. Color version available in the online PDF.

Table 3. List of the buckets that discriminate the fatty livers before (at 20 min postmortem, n = 25) and after chilling (at 6 h postmortem, n = 24; variable importance in projection (VIP) >2)[1]

Chemical shift	Metabolite	HMDB annotation	Multiplet[2]	Ratio[3]	VIP	P[4]
3.655	Glycerol	HMDB00131	m	2.14	4.81	***
3.965	Serine	HMDB00187	m	1.53	3.29	***
3.975	Serine	HMDB00187	m	1.69	2.95	***
3.855	Glucose/serine	HMDB00122/HMDB00187	m	1.48	5.11	***
3.445	Glucose	HMDB00122	m	1.46	2.56	***
3.675	Glucose	HMDB00122	m	1.3	3.37	***
3.695	Glucose	HMDB00122	m	1.27	3.08	***
3.715	Glucose	HMDB00122	m	1.21	3.49	***
3.725	Glucose	HMDB00122	m	1.22	3.06	***
3.735	Glucose	HMDB00122	m	1.19	3.04	***
3.825	Glucose	HMDB00122	m	1.15	2.27	***
3.835	Glucose	HMDB00122	m	1.25	4.42	***
3.845	Glucose	HMDB00122	m	1.39	4.33	***
3.865	Glucose	HMDB00122	m	1.76	4.15	***
3.875	Glucose	HMDB00122	m	1.33	2.83	***
5.235	Glucose	HMDB00122	d	1.25	3.18	***
3.765	Glucose, alanine, glutamine, glutathione, glutamate	HMDB00122/HMDB00161 /HMDB00641/HMDB00129 /HMDB00148	m	1.27	3.43	***
3.775	Glucose, alanine, glutamine, glutathione, glutamate	HMDB00122/HMDB00161 /HMDB00641/HMDB00129 /HMDB00148	m	1.19	3.51	***
3.785	Glucose, alanine, glutamine, glutathione, glutamate	HMDB00122/HMDB00161 /HMDB00641/HMDB00129 /HMDB00148	m	1.2	3.02	***
3.415	Glucose, taurine, proline	HMDB00122/HMDB00251 /HMDB00162	m	1.09	2.04	***
3.425	Glucose, taurine, proline	HMDB00122/HMDB00251 /HMDB00162	m	1.28	3.43	***
3.565	Glycerol	HMDB00131	m	1.34	2.72	***
3.575	Glycerol	HMDB00131	m	1.37	2.69	***
3.635	Glycerol	HMDB00131	m	1.35	3.26	***
3.645	Glycerol	HMDB00131	m	1.56	4.58	***
3.795	Glycerol	HMDB00131	m	1.21	2.07	***
3.745	Lysine	HMDB00182	m	1.15	2.11	***
3.755	Lysine	HMDB00182	m	1.16	2.34	***
3.585	Myo-inositol	HMDB00211	m	2.99	4.46	***
3.595	Myo-inositol	HMDB00211	m	1.8	3.61	***
3.605	Myo-inositol	HMDB00211	m	1.16	2.28	***
3.615	Myo-inositol	HMDB00211	m	1.19	2.27	***
3.205	Choline	HMDB00097	s	1.34	2.12	***
3.945	Betaine	HMDB00043	s	1.32	2.28	***
3.265	Taurine, betaine	HMDB00251/HMDB00043	t/s	0.87	2.13	***
2.415	Succinate	HMDB00254	s	0.75	3.13	***
1.325	Lactate	HMDB01311	d	0.8	4.33	***
1.335	Lactate	HMDB01311	d	0.8	4.36	***
4.105	Lactate	HMDB01311	q	0.76	2.2	***
4.115	Lactate	HMDB01311	q	0.75	2.52	***
4.125	Lactate, proline	HMDB01311/HMDB00163	q/q	0.71	2.28	***
4.055	Choline, myo-inositol	HMDB00097/HMDB00211	t	0.64	2.52	***
4.065	Choline, myo-inositol	HMDB00097/HMDB00211	t	0.74	2.26	***
3.235	Glycerophosphocholine	HMDB00086	s	0.77	5.56	***
4.325	Glycerophosphocholine	HMDB00086	m	0.65	2.12	***
4.335	Glycerophosphocholine	HMDB00086	m	0.68	2.06	***
3.225	Phosphocholine		s	0.69	6.68	***
2.165	Glutamine, glutathione	HMDB00641/HMDB00125	m	0.64	2.25	***
2.175	Glutamine, glutathione	HMDB00641/HMDB00125	m	0.55	2.25	***
4.385	ATP	HMDB00538	s	0.27	2.01	***
4.375	Uridine	HMDB00296	q	0.24	2.29	***

[1]The R^2Y and Q^2 values of the model were 0.978 and 0.968, respectively; HMDB = Human Metabolome Database.

[2]Multiplet indicates the peak form on the ^{1}H-NMR spectra, s for singlet, d for doublet, t for triplet, and m for multiplet.

[3]Ratio represents the 6 h postmortem to 20 min postmortem and the fatty livers sampled at 20 min postmortem.

[4]P is the FDR corrected P-value of the ANOVA of the fat loss group effect.

***$P < 0.001$.

than 2 for the other buckets. The ratios were around 0.70 (Table 3). The diminution of these metabolites could be related to the stop of phospholipid synthesis.

The ATP with the bucket at 4.385 ppm had a VIP value of 2.01, but it had a very weak ratio (0.27) (Table 3). Théron et al. (2013) showed that the ATP synthase

subunit β was strongly decreased during the chilling. This is in accordance with PM processes: ATP was consumed by cells to maintain their metabolism, then, little by little, the lack of ATP storage caused the arrest of cell metabolism. The molecule of succinate had only one singlet peak that corresponds to the bucket at 2.415 ppm. Its VIP value was 3.13 and its ratio was 0.75 (Table 3). The succinate is mainly involved in aerobic processes in Krebs cycle. The PM anaerobic conditions probably led to the diminution of aerobic cell metabolism in liver, as suggested by the variations in the succinate content.

The ^{1}H-NMR analysis of the fatty liver allowed acquiring new data on the hydrophilic profile of fatty livers. This study evidences that ATP amount in liver cells is strongly reduced during PM evolution. The lipolysis of triglycerides seems to be enhanced during this step. In liver, glycogen is converted into glucose but glucose is not converted into lactate, contrary to muscles.

The main results of this study show that the high-fat-loss livers are more advanced in PM processes than low-fat-loss livers at 20 min PM. The accelerated PM processes (with hydrolysis of carbohydrate storage, worse membrane integrity, and higher catabolic processes) are probably the causes of the differences in fat loss during cooking.

ACKNOWLEDGMENTS

REFERENCES

Barak, A. J., H. C. Beckenhauer, S. Badakhsh, and D. J. Tuma. 1997. The effect of betaine in reversing alcoholic steatosis. Alcohol. Clin. Exp. Res. 21:1100–1102.

Baudonnet-Lenfant, C., A. Auvergne, and R. Babilé. 1991. Influence de la durée de jeûne avant l'abattage et du poids à la mise en gavage des canards de Barbarie sur la composition chimique hépatique. Annat Zoot 40:161–170.

Beach, D. C., and P. K. Flick. 1982. Early effect of myo-inositol deficiency on fatty acid synthetic enzymes of rat liver. Biochim. Biophys. Acta 711:452–459.

Beckonert, O., H. C. Keun, T. M. D. Ebbels, J. Bundy, E. Holmes, J. C. Lindon, and J. K. Nicholson. 2007. Metabolic profiling, metabolomic and metabonomic procedures for NMR spectroscopy of urine, plasma, serum and tissue extracts. Nat. Protoc. 2:2692–2703.

Bendall, J. R. 1979. Relations between muscle pH and important biochemical parameters during the postmortem changes in mammalian muscles. Meat Sci. 3:143–157.

Bergmeyer, H. 1974. Methods of Enzymatic Analysis. G. H. Bourne, ed. Academic Press, New York, NY.

Blum, J., C. Labie, and P. Raynaud. 1990. Influence du poids et de la composition chimique du foie gras d'oie sur la fonte mesurée après stérilisation à 104°C. Sci. Aliments 10:543–554.

Bouillier-Oudot, M., S. Leprettre, J. Dubois, and R. Babilé. 2002. Itinéraires post-mortem et caractéristiques technologiques et organoleptiques des foies gras d'oies.Pages 172–175 in 5e Journees de la Recherche des Palmipèdes a Foie Gras, Pau, France.

Cazeils, J. L., M. Bouillier-Oudot, A. Auvergne, M. Candau, and R. Babile. 1999. Lipid composition of hepatocyte plasma membranes from geese overfed with corn. Lipids 34:937–942.

Chartrin, P., M.-D. Bernadet, G. Guy, J. Mourot, J.-F. Hocquette, N. Rideau, M. J. Duclos, and E. Baéza. 2006. Does overfeeding enhance genotype effects on liver ability for lipogenesis and lipid secretion in ducks? Comp. Biochem. Physiol. A Mol. Integr. Physiol. 145:390–396.

Croze, M. L., R. E. Vella, N. J. Pillon, H. A. Soula, L. Hadji, M. Guichardant, and C. O. Soulage. 2013. Chronic treatment with myo-inositol reduces white adipose tissue accretion and improves insulin sensitivity in female mice. J. Nutr. Biochem. 24:457–466.

Dalrymple, R. H., and R. Hamm. 1973. A method for the extraction of glycogen and metabolites from a single muscle sample. Int. J. Food Sci. Technol. 8:439–444.

Evans, Z. P., B. S. Mandavilli, J. D. Ellett, D. Rodwell, M. W. Fariss, R. N. Fiorini, R. G. Schnellmann, M. G. Schmidt, and K. Chavin. 2009. Vitamin E succinate enhances steatotic liver energy status and prevents oxidative damage following ischemia/reperfusion. Transplant. Proc. 41:4094–4098.

Fernandez, X., M. Bouillier-Oudot, C. Molette, M. D. Bernadet, and H. Manse. 2011. Duration of transport and holding in lairage at constant postprandial delay to slaughter: Effects on fatty liver and breast muscle quality in mule ducks. Poult. Sci. 90:2360–2369.

Folch, J., M. Lees, and G. H. Sloane Stanley. 1957. A simple method for the isolation and purification of total lipids from animal tissues. J. Biol. Chem. 226:497–509.

Hochberg, Y., and Y. Benjamini. 1990. More powerful procedures for multiple significance testing. Stat. Med. 9:811–818.

JOCE. 1971. Journal Officiel des Communautés Européennes. Dosage de l'humidité. JOCE L279/8. Eur-Op News, Luxembourg.

JORF. 1993. Journal Officiel de la République Française. Décret n°93–9-99 du 09–08–93 du JO du 14–08–93, relatif aux préparations à base de foie gras.

JORF. 2006. Journal Officiel de la République Française. Code Rural français, Article L654–27–1, Created by the Loi n°2006–11 du 5 janvier 2006, art. 74 JORF 6 janvier 2006.

Klein, M., C. Dorn, M. Saugspier, C. Hellerbrand, P. Oefner, and W. Gronwald. 2011. Discrimination of steatosis and NASH in mice using nuclear magnetic resonance spectroscopy. Metabolomics 7:237–246.

Kondo, T., M. Kishi, T. Fushimi, and T. Kaga. 2009. Acetic acid upregulates the expression of genes for fatty acid oxidation enzymes in liver to suppress body fat accumulation. J. Agric. Food Chem. 57:5982–5986.

Latil, G., A. Auvergne, and R. Babilé. 1996. Consommation du canard mulard en gavage. Relation avec les performances zootechniques et la qualité du foie gras. Pages 93–97 in 2eme Journees de la Recherche sur les Palmipedes a Foie Gras, Bordeaux, France.

Lopez-Bote, C. J., F. Toldrá, A. Daza, J. M. Ferrer, D. Menoyo, L. Silió, and M. C. Rodríguez. 2008. Effect of exercise on skeletal muscle proteolytic enzyme activity and meat quality characteristics in Iberian pigs. Meat Sci. 79:71–76.

Marie-Etancelin, C., B. Basso, S. Davail, K. Gontier, X. Fernandez, Z. G. Vitezica, D. Bastianelli, E. Baéza, M.-D. Bernadet, G. Guy, J.-M. Brun, and A. Legarra. 2011. Genetic parameters of product quality and hepatic metabolism in fattened mule ducks. J. Anim. Sci. 89:669–679.

Neuschwander-Tetri, B. A. 2001. Betaine: An old therapy for a new scourge. Am. J. Gastroenterol. 96:2534–2536.

Rousselot-Pailley, D., G. Gérard, D. Gourichon, N. Sellier, and J. Blum. 1992. Influences des conditions d'abattage et de réfrigération sur la qualité des foies gras d'oie. INRA Prod. Anim. 5:167–172.

Sharp, J. G. 1935. Post mortem breakdown of glycogen and accumulation of lactic acid in fish-muscle at low temperatures. Biochem. J. 29:850–853.

Théron, L., T. Astruc, M. Bouillier-Oudot, C. Molette, A. Vénien, F. Peyrin, Z. Vitezica, and X. Fernandez. 2011a. The fusion of lipid droplets is involved in fat loss during cooking of duck "foie gras." Meat Sci. 89:377–383.

Théron, L., M. Cullere, M. Bouillier-Oudot, H. Manse, A. Dalle Zotte, C. Molette, X. Fernandez, and Z. G. Vitezica. 2012. Modeling the relationships between quality and biochemical composition of fatty liver in mule ducks. J. Anim. Sci. 90:3312–3317.

Théron, L., X. Fernandez, N. Marty-Gasset, C. Chambon, D. Viala, C. Pichereaux, M. Rossignol, T. Astruc, and C. Molette. 2013. Proteomic analysis of duck fatty liver during post-mortem storage related to the variability of fat loss during cooking of "foie gras." J. Agric. Food Chem. 61:920–930.

Théron, L., X. Fernandez, N. Marty-Gasset, C. Pichereaux, M. Rossignol, C. Chambon, D. Viala, T. Astruc, and C. Molette. 2011b. Identification by proteomic analysis of early post-mortem markers involved in the variability in fat loss during cooking of mule duck "foie gras." J. Agric. Food Chem. 59:12617–12628.

Yamamoto, H., T. Aikawa, H. Matsutaka, T. Okuda, and E. Ishikawa. 1974. Interorganal relationships of amino acid metabolism in fed rats. Am. J. Physiol. 226:1428–1433.

Yamashita, H., H. Maruta, M. Jozuka, R. Kimura, H. Iwabuchi, M. Yamato, T. Saito, K. Fujisawa, Y. Takahashi, M. Kimoto, M. Hiemori, and H. Tsuji. 2009. Effects of acetate on lipid metabolism in muscles and adipose tissues of type 2 diabetic Otsuka Long-Evans Tokushima Fatty (OLETF) rats. Biosci. Biotechnol. Biochem. 73:570–576.